

Metasomatized hazburgite xenoliths from Avacha volcano as fragments of mantle wedge of the Kamchatka arc: Implication for the metasomatic agent

メタデータ	言語: eng 出版者: 公開日: 2017-10-03 キーワード (Ja): キーワード (En): 作成者: メールアドレス: 所属:
URL	https://doi.org/10.24517/00010738

This work is licensed under a Creative Commons Attribution-NonCommercial-ShareAlike 3.0 International License.



Thematic Article

Metasomatized harzburgite xenoliths from Avacha volcano as fragments of mantle wedge of the Kamchatka arc: Implication for the metasomatic agent

SHOJI ARAI,^{1,*} SATOKO ISHIMARU¹ AND VICTOR M. OKRUGIN²

¹Department of Earth Sciences, Kanazawa University, Kanazawa 920-1192, Japan (email: ultrasa@kenroku.kanazawa-u.ac.jp) and ²Department of Physical-Chemical Methods of Research and Mineralogy, Institute of Volcanology, Russian Academy of Science, 683006, Petropavlovsk-Kamchatsky, Russia

Abstract Abundant peridotite xenoliths have been found in pyroclastics of Avacha (Avachinsky) volcano, the south Kamchatka arc, Russia. They are mostly refractory harzburgite with or without clinopyroxene: the Fo of olivine and Cr/(Cr + Al) atomic ratio of spinel range from 91 to 92 and from 0.5 to 0.7, respectively. They are metasomatized to various extents, and the metasomatic orthopyroxene has been formed at the expense of olivine. The metasomatic orthopyroxene, free of deformation and exsolution, is characterized by low contents of CaO and Cr₂O₃. The complicated way of replacement possibly indicates low viscosity of the metasomatic agent, namely hydrous fluids released from the relatively cool slab beneath the south Kamchatka arc. This is a good contrast to the north Kamchatka arc, where the slab has been hot enough to provide slab-derived melts. High content of total orthopyroxene, 40 vol% on average, in metasomatized harzburgite from Avacha suggests silica enrichment of the mantle wedge, and is equivalent to some subcratonic harzburgite. Some subcratonic harzburgites therefore could have been formed by transportation of subarc metasomatized peridotites to a deeper part of the upper mantle.

Key words: harzburgite, Kamchatka arc, mantle wedge, metasomatism, orthopyroxene, silica enrichment, slab-derived fluid.

INTRODUCTION

Peridotite xenoliths are fragments of the upper mantle and they provide direct information on deep materials and processes, and have been attracting the attention of petrologists to date (Ross *et al.* 1954). Their derivation has been rather limited in terms of tectonic setting to continental areas (rift zones and cratons) and oceanic hotspots (Nixon 1987). Peridotite xenoliths derived from possible mantle wedge overlying slab have been reported from several arcs, that is, from Japan arcs (Takahashi 1978; Aoki 1987; Arai *et al.* 1998), the Luzon arc (Maury *et al.* 1992; Schiano *et al.*

1995; Arai & Kida 2000), the Kamchatka arc (Koloskov & Khotin 1978; Kepezhinskias *et al.* 1995;), the Colorado Plateau (Smith & Riter 1997; Smith 2000), the Cascade Range, USA (Brandon & Draper 1996; Ertan & Leeman 1996), Mexico (Luhr & Aranda-Gomez 1997; Blatter & Carmichael 1998) and the Tabar–Lihir–Tanga–Feni (TLTF) arc, Papua New Guinea (McInnes *et al.* 2001; Franz *et al.* 2002).

Peridotite xenoliths carried by arc magmas are especially important because of their genuine subarc character and have been reported from several arcs (e.g. Kamchatka, Luzon and Papua New Guinea), in addition to the classical example of the Ichinomegata crater of Megata volcano, the North-east Japan arc. Among them peridotite xenoliths from Avacha volcano of the south Kamchatka arc have large amounts of secondary ortho-

*Correspondence.

pyroxene, and we can analyze the metasomatic process for its formation relatively easily. Peridotite xenoliths from the north Kamchatka arc (Kepezhinskas *et al.* 1995, 1996) are very different from those from Avacha volcano in that the former were metasomatized by the melt to produce Al-augite series ultramafic rocks. The Avacha peridotite is unique in having orthopyroxene as the main metasomatic mineral, being different from peridotites from Iraya and the TLTF arc, which commonly have amphibole and phlogopite with the secondary orthopyroxene (Arai & Kida 2000; McInnes *et al.* 2001). The Avacha volcano also has an advantage in providing a large amount of peridotite xenoliths (Shcheka 1976). We intend to describe the petrographic and petrologic characteristics of the peridotite xenoliths from Avacha volcano in order to understand the upper mantle processes beneath an arc volcano.

GEOLOGICAL BACKGROUND

Avacha (Avachinsky) volcano is located at 53°15.3'N and 158°49.8'E on the volcanic front of the southern Kamchatka arc, and is close to the city of Petropavlovsk-Kamchatsky (Fig. 1). The Pacific plate subducts beneath the Kamchatka Peninsula at a rate of 9 cm/year through a trench approximately 200 km off the coast, and the depth to the slab is approximately 100–120 km beneath Avacha volcano (Tatsumi *et al.* 1994). Avacha volcano has been one of the most active volcanoes of the Kamchatka arc during the 18th–20th centuries (Ivanov *et al.* 1996).

The eruption of Avacha volcano has been known to be sometimes explosive and catastrophic: many large-scale lahars were discovered both in historic and prehistoric eruptions (Melekestsev *et al.* 1996). The Avacha volcano has been active from the late Pleistocene, and the volcanic activity during the Holocene can be divided into two stages, I Av (from 7200 to 3700 years BP) and II Av (3500 years BP; Braitseva *et al.* 1998). The magma is andesite for I Av and basaltic andesite for II Av. The 1991 eruption is characterized by the highest ($\text{SiO}_2 + \text{K}_2\text{O}$) contents of the magma during the last 3000–4000 years (Ivanov *et al.* 1996). Twenty-seven explosive eruptions have been found at I Av stage, and several of them provided peridotite xenoliths to the surface (Braitseva *et al.* 1998). The volcanic products of the I Av stage were pyroclastic flows composed of vesicular andesite blocks and pumice, which are pale-colored and contain small

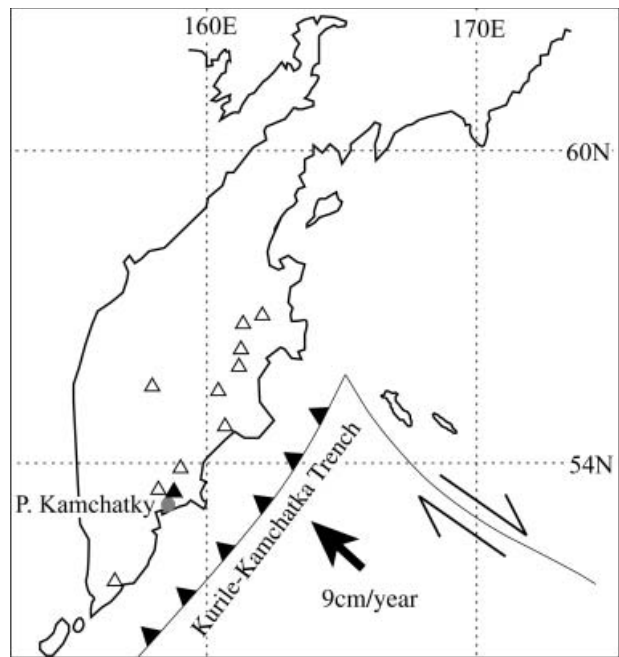


Fig. 1 Location of Avacha volcano on the Kamchatka Peninsula. (Δ), volcano that produces peridotite xenoliths (after Koloskov & Khotin 1978).

amounts of K_2O and 58–61 wt% of SiO_2 . The volcanics of Avacha volcano are distinctive from those of adjacent volcanoes in their precipitation of hornblende and low K content (Braitseva *et al.* 1998).

Several pyroclastic deposits have been found to contain ultramafic xenoliths: pyroclastics of I Av15 (*ca* 5200 years BP), I Av16 (*ca* 5000 years BP) and I Av24 (*ca* 4000 years BP; Braitseva *et al.* 1998). Among them the I Av24 deposits are well known to contain abundant xenoliths of harzburgite, clinopyroxenite and hornblende gabbro. Peridotite xenoliths used in the present study were obtained from a secondary debris deposit attributed to a small sector collapse, which presumably contains pyroclastics from I Av16 and I Av24.

PETROGRAPHY

HOST ROCK

Host rock for the peridotite xenoliths is basaltic andesite, containing phenocrysts or microphenocrysts of olivine, plagioclase, hornblende, hypersthene, augite and titanomagnetite. Olivine, rounded to euhedral in shape, sometimes contains minute opaque spinel inclusions, and often forms crystal aggregates with or without clinopyroxene. Plagioclase is usually euhedral and is strongly

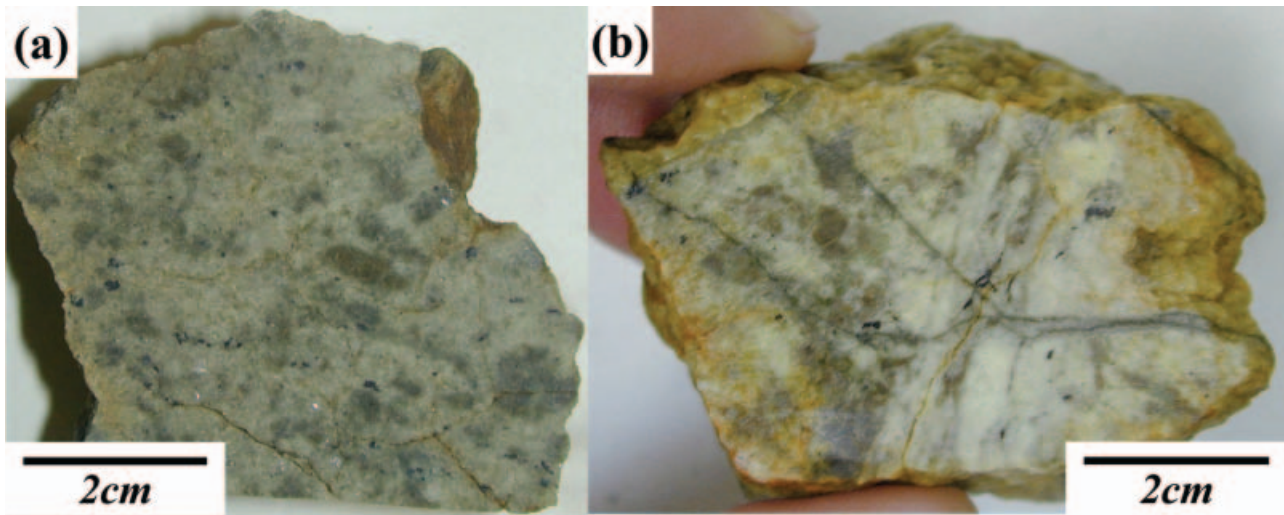


Fig. 2 Photographs of peridotite xenoliths from Avacha, the Kamchatka arc. (a) Coarse-grained primary harzburgite with least degree of metasomatism. Grayish green spots are orthopyroxene, and olivine mainly comprises the yellowish part. Black dots are chromian spinel. Note that there are no emerald green spots of clinopyroxene. (b) Fine-grained peridotite that underwent intense metasomatism and shearing. Grayish speckles are due to concentration of minute spinel grains.

zoned. It sometimes has a dusty core and clear rim. Plagioclase also forms crystal aggregates with pyroxenes and magnetite. Hornblende is euhedral and has light greenish brown to light yellowish brown pleochroism. Hypersthene and augite tend to be smaller in size than other silicate phenocrysts. The groundmass has an intergranular texture.

PERIDOTITE XENOLITHS

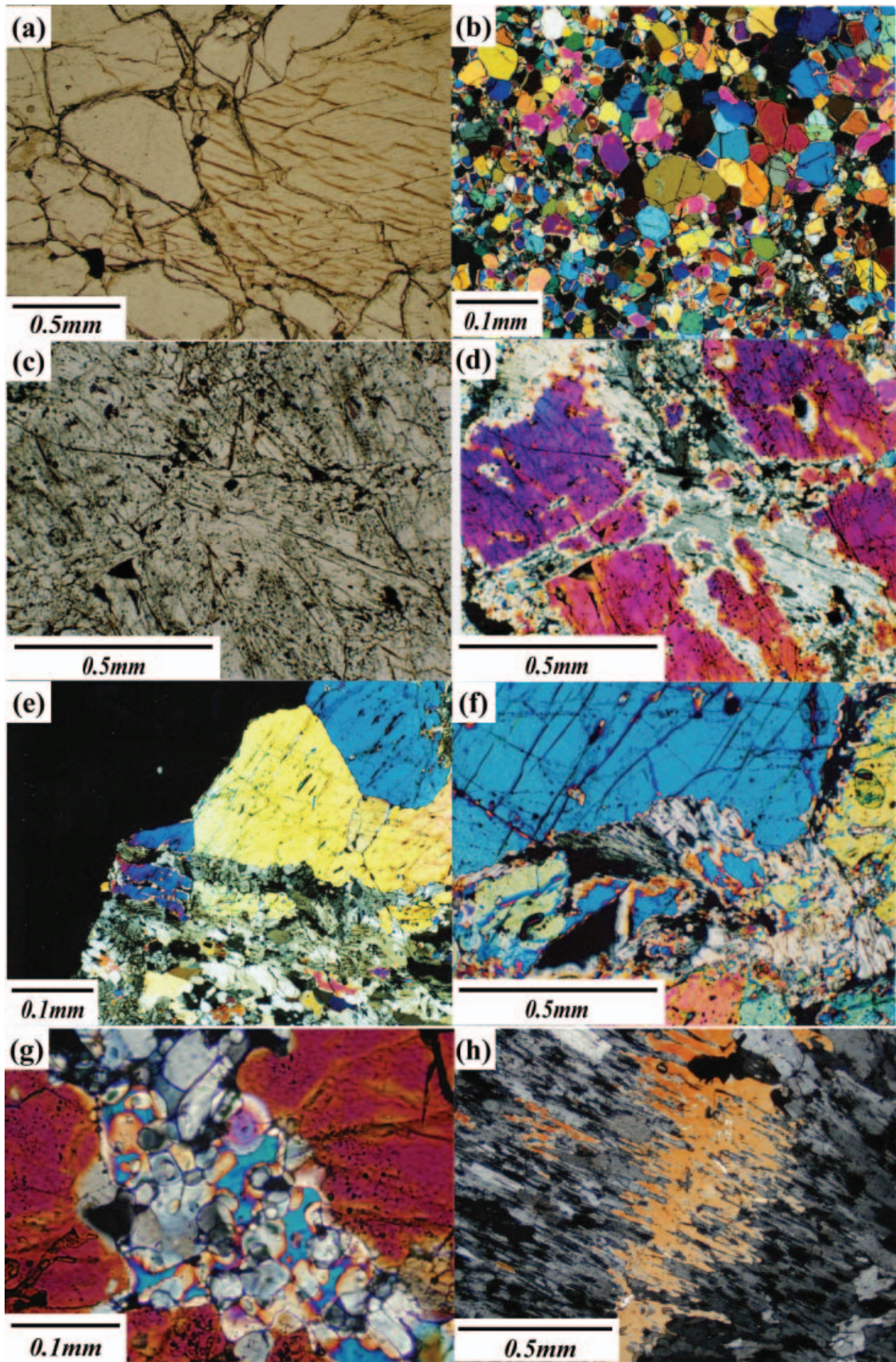
The peridotite xenoliths are most frequently 5 cm and are up to 25 cm across. Harzburgite is most abundant, and pyroxenites (clinopyroxenite and orthopyroxenite), dunite and gabbroic rocks are found only subordinately. The peridotite xenoliths are various in grain size both within individual pieces and from piece to piece (Fig. 2). The fine-grained peridotites are paler in color than the coarse granular ones (Fig. 2). Pyroxenites are found both as bands or layers in harzburgite and as discrete xenoliths. Typical microscopic characteristics of peridotites are shown in Figs 3 and 4.

The peridotite xenoliths are frequently covered with or cut by thin hornblendite, up to 5 mm (mostly 1 mm) in thickness. Clinopyroxene was precipitated along the hornblende selvage on the inner peridotite side. Peridotite is occasionally in direct contact with the host andesite, where orthopyroxene in peridotite is intact and exhibits no reaction with the andesitic melt. The presence or

absence and thickness of the hornblendite selvage are totally independent from any textural and lithological characteristics of peridotite xenoliths. The peridotite xenoliths evenly suffer from chemical modification only within several millimeters from the contact with hornblendite. The selvage and veinlet of hornblendite or gabbros are common to some peridotite xenoliths carried by arc-type calc-alkaline andesites, for example the Iraya volcano, the Luzon arc (Arai *et al.* 1996) and Oshima-Oshima volcano, the North-east Japan arc (Ninomiya & Arai 1992).

Primary peridotite

Harzburgite is coarse-grained, and usually exhibits protogranular to porphyroclastic textures with coarse olivine and orthopyroxene grains of up to 1 cm across in some samples (Fig. 3a). Olivine and orthopyroxene with exsolution lamellae of clinopyroxene are commonly kinked. Clinopyroxene is smaller in size and is closely associated with orthopyroxene even if it occurs as discrete grains. Chromian spinel is subhedral to anhedral and exhibits a black to reddish brown color under the microscope (Fig. 3a). Chromian spinel commonly occurs as thin lamellae in coarse olivine grains. Olivine and orthopyroxene are 54–88% and 40–10%, respectively, in volume (Fig. 5). As described in the following section, secondary orthopyroxene and other metasomatic minerals are contained in various amounts in harzburgite.



Dunitic peridotite is basically fine-grained equigranular, being characterized by strain-free olivine grains, 0.1–0.5 mm across in size (Fig. 3b). Grain boundaries are curvilinear and have clear triple junctions. Olivine is less turbid with small amount of inclusions in dunite (Fig. 3b) than in harzburgite. Chromian spinel has been stretched to fine-grained aggregates, which are often associated with hornblende.

Metasomatized peridotite

The primary harzburgite has been modified to various degrees by a metasomatic agent. Metasomatic secondary minerals are predominantly orthopyroxene, and very subordinately hornblende and clinopyroxene. Secondary orthopyroxene cuts olivine in various ways: it replaces olivine in very complicated ways (Fig. 3c,d) or it cross-cuts olivine as a veinlet (Fig. 3e). In the latter case, the boundary of wall olivine is ragged, indicating replacement. The shape of orthopyroxene varies from a small rounded crystal (<0.1 mm across) to a large prismatic one. The prismatic orthopyroxene commonly exhibits characteristically radial aggregates similar to that in the metasomatized xenoliths from Iraya volcano, the Luzon arc (Arai & Kida 2000; Fig. 3f). The rounded fine orthopyroxene of secondary origin is usually associated with rounded fine olivine and interstitial glass that is colorless and isotropic, or hornblende (Fig. 3g). In addition to the morphological difference, the secondary orthopyroxene is completely free from deformation or kinking and the clinopyroxene exsolution that are common in primary orthopyroxene. No phlogopite has been found.

Primary coarse orthopyroxene has often been recrystallized to fine secondary grains along grain boundaries and cracks (Fig. 3h). The recrystallization zone is commonly continuous to secondary orthopyroxene veinlets cutting olivine. Clinopyroxene lamellae have been occasionally coarsened or hydrated to form hornblende (Fig. 3h).

The secondary orthopyroxene due to reaction of olivine with a metasomatic agent can be thus clas-

sified into three types. The first is olivine-replacing orthopyroxene with prismatic or radiating forms without associated glass and/or hornblende (Fig. 3c–f). The second is olivine-replacing orthopyroxene with small stout or rounded forms associated with glass and/or hornblende (Fig. 3g). The third is recrystallized primary orthopyroxene as aforementioned (Fig. 3h).

Primary olivine, even if apparently intact from metasomatism, is usually rich in minute inclusions and exsolutions, giving the rock a turbid appearance in thin section (Fig. 3c). Lamellar chromian spinel is very common in the metasomatized harzburgite. Rounded or oval inclusions composed of glass and minute crystals are also common. Minute grains of chromian spinel and, less frequently, sulfide are scattered both in olivine and orthopyroxene of secondary origin.

The amount of total orthopyroxene is mostly around 40 vol% in the metasomatized harzburgite with secondary orthopyroxene. It is noteworthy that the metasomatized harzburgite has a higher amount of total orthopyroxene than the primary harzburgite (Fig. 5), indicating an increase of total orthopyroxene volume during the metasomatism.

Fine-grained peridotite

Approximately 15% of all peridotite xenoliths examined partly or wholly have fine-grained textures mainly composed of minute (<0.1 mm across) grains of olivine (Fig. 4a,b). The fine-grained part of peridotite frequently has pale brownish speckles several millimeters across, which are fine-grained olivine and orthopyroxene with minute chromian spinel inclusions as mentioned in the following section (Fig. 4c). Primary chromian spinel is stretched (Fig. 4a), and is usually recrystallized into fine-grained aggregates. The fine-grained peridotite from Avacha is very similar in appearance to F-type peridotite from Iraya volcano, the Luzon arc (Arai *et al.* 1996; Arai & Kida 2000).

The fine-grained peridotite has textures somewhat similar to mylonites but symmetrical porphyroclasts, which suggest rotation during shearing

Fig. 3 Photomicrographs of primary and metasomatized peridotites from Avacha. Crossed-polarized light if not otherwise stated. (a) Primary harzburgite with porph roclastic texture. Large porphyroclast with cleavage at the right half is orthopyroxene and small black grain is chromian spinel. Plane-polarized light. (b) Dunite with fine-grained equigranular texture. Note that olivine is not strained. (c) Coarse primary olivine replaced by metasomatic olivine in a complicated way in a highly metasomatized harzburgite. Note the turbid appearance due to minute inclusions. Plane-polarized light. (d) Same as (c). Note the very complicated boundaries between olivine (reddish) and metasomatic orthopyroxene (gray). (e) Primary olivine cut by veinlets of metasomatic orthopyroxene (gray) in a metasomatized harzburgite. (f) Primary olivine embayed by metasomatic orthopyroxene (gray) in a complicated way in a metasomatized harzburgite. Note the radial aggregate of orthopyroxene. (g) Primary olivine partly replaced by fine-grained metasomatic orthopyroxene (gray) with interstitial hornblende (blue) and glass (black). (h) Primary orthopyroxene completely recrystallized to be fine-grained aggregate of secondary orthopyroxene (gray) by the metasomatic agent. Clinopyroxene lamella is coarsened (center, orange).

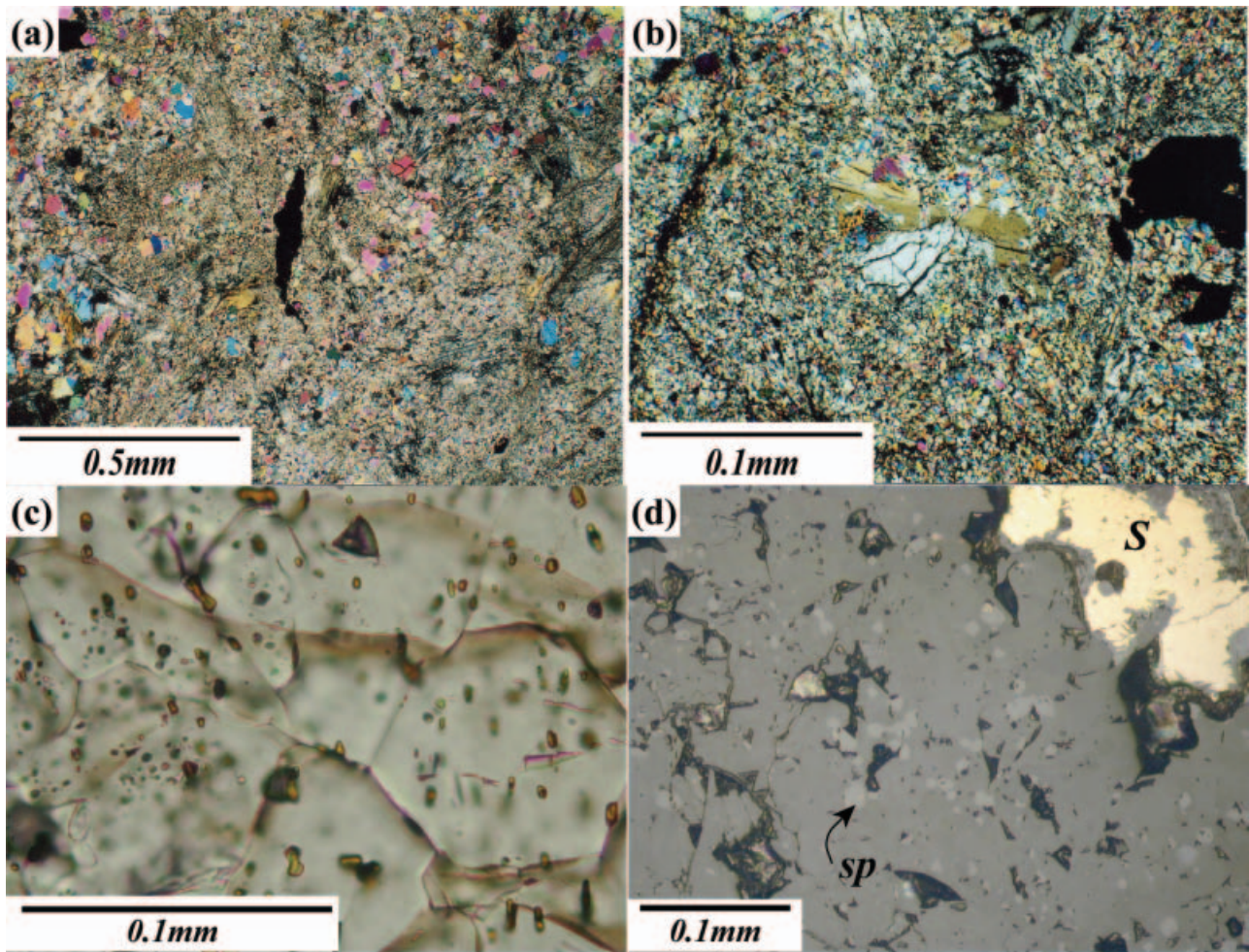


Fig. 4 Photomicrographs of fine-grained peridotites from Avacha. (a) Fine-grained dunitic peridotite mainly composed of extremely fine-grained olivine. Coarser strain-free olivine grains are scattered. Center is stretched chromian spinel (black). Plane-polarized light. (b) Fine-grained peridotite composed of extremely fine-grained matrix of olivine and orthopyroxene and coarser grains of secondary orthopyroxene (center) and chromian spinel (central right, black). Crossed-polarized light. (c) Relatively fine-grained part composed of olivine in a slightly metasomatized and sheared harzburgite. Note the numerous minute inclusions of chromian spinel. Plane-polarized light. (d) Fine-grained section mainly composed of recrystallized rounded olivine in a metasomatized harzburgite. Lighter gray spots are chromian spinel inclusions (sp.). Note the frequent occurrence of sulfide (S). Reflected light.

characteristic of mylonitization, have not been found. The peridotite is composed of a fine-grained aggregate of olivine and orthopyroxene with minute rounded chromian spinel (Fig. 4c). Hornblende is associated with olivine and orthopyroxene in some samples. Medium grains of olivine, which is turbid or clear, are commonly associated with orthopyroxene of secondary origin in the fine-grained matrix (Fig. 4b). The clear olivine is subhedral to anhedral, and is commonly embedded in medium turbid olivine. The matrix olivine is extremely fine ($<10\mu\text{m}$ across) and rounded in shape in some samples. Sulfide is common in the fine-grained part (Fig. 4d).

MINERAL CHEMISTRY

Minerals were analyzed by a JEOL wavelength dispersive electron probe X-ray microanalyzer (JXA8800) at the Center for Co-operative Research of Kanazawa University. Analytical conditions were 15-kV accelerating voltage, 0.4-mA probe current and 3- μm probe diameter. The 20-kV accelerating voltage and 0.67-mA probe current were adopted in Ni analysis of olivine. Ferrous and ferric iron contents of chromian spinel were calculated assuming spinel stoichiometry. Cr# is the Cr/(Cr + Al) atomic ratio of chromian spinel. Mg# is the Mg/(Mg + total Fe) atomic ratio

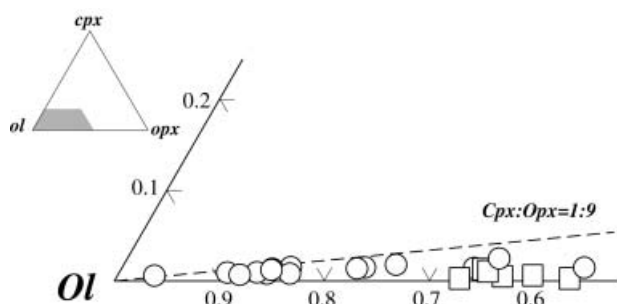


Fig. 5 Modal amounts of olivine, orthopyroxene and clinopyroxene in coarse-grained peridotites from Avacha. Note that the metasomatized harzburgite has a higher content of total orthopyroxene, 40 vol% on average. (○), primary; (□), metasomatized.

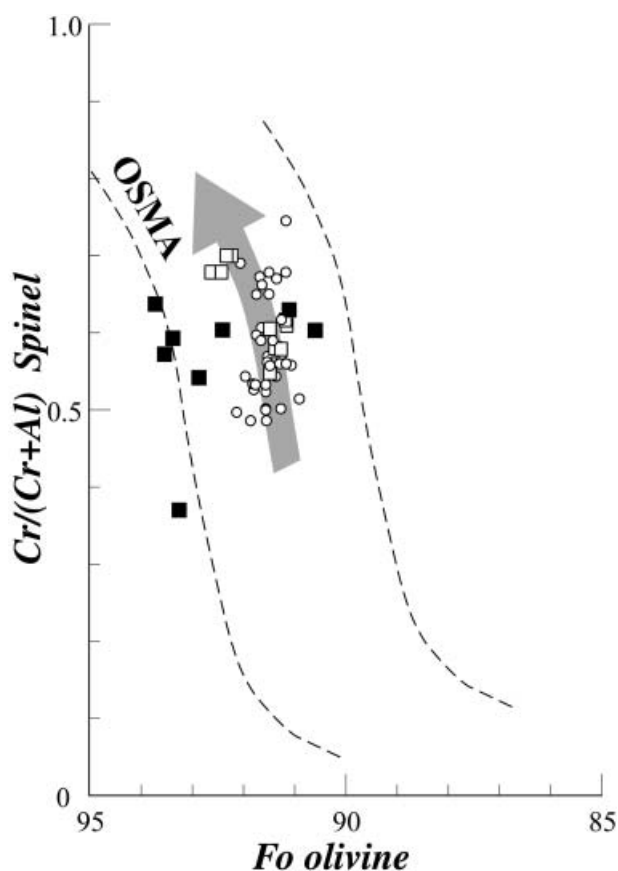


Fig. 6 Relationships between the Fo content of olivine and Cr# of chromian spinel in peridotite xenoliths from Avacha. (○), primary, unmetasomatized peridotite; (□), metasomatized, metasomatized peridotite with secondary orthopyroxene; (■), fine-grained, fine-grained recrystallized peridotite. Note the pairs from primary unmetasomatized harzburgites denote a residual trend (thick gray line with arrow) within the olivine–spinel mantle array (OSMA; Arai 1994a), and that the Fo content of olivine is variable in highly metasomatized fine-grained peridotites.

for silicates and also the $Mg/(Mg + Fe^{2+})$ atomic ratio for chromian spinel. Selected microprobe analyses are listed in Table 1.

Olivine is mostly Fo_{91-92} in composition for unmetasomatized harzburgite (Fig. 6). Harzburg-

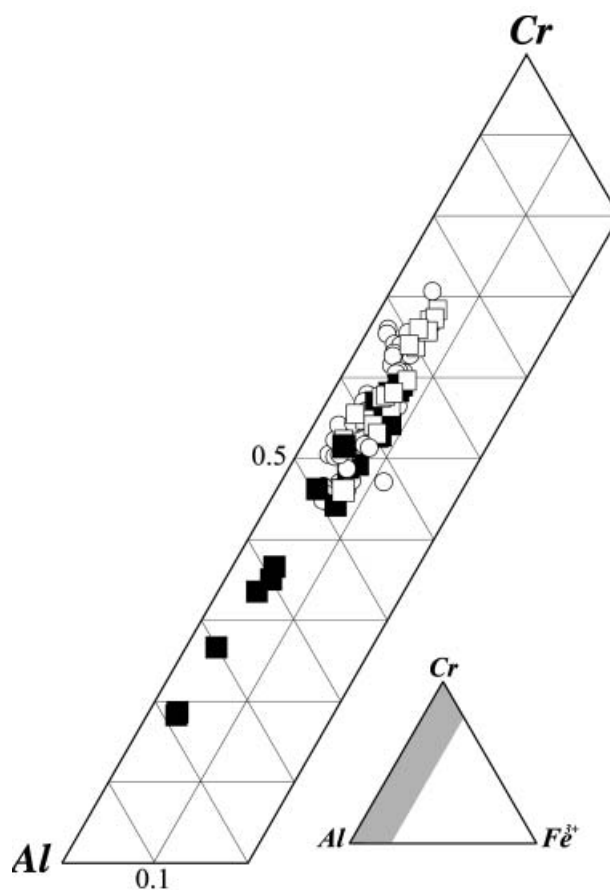


Fig. 7 Trivalent cation ratios of chromian spinels in peridotite xenoliths from Avacha. (○), primary; (□), metasomatized; (■), fine-grained.

ite from Avacha is plotted within the olivine–spinel mantle array, which is a spinel peridotite restite trend in terms of olivine–spinel compositional relation (Arai 1994a; Fig. 6). Dunite is included in the harzburgite range for the olivine–spinel compositional relation. The Cr# of chromian spinel does not show a positive correlation with the Fo content of coexisting olivine in primary peridotites (Fig. 6). Both olivine and spinel compositions are highly variable without correlation in recrystallized fine-grained peridotites (Fig. 6) although only two samples have been analyzed. Olivine is Fe-rich (down to $Fo_{81.6}$) within several millimeters from the hornblende selvage.

The Cr# of coarse primary chromian spinel ranges from 0.5 to 0.7 in harzburgite except for the fine-grained spinel (Figs 6,7). Minute spinel from aggregates that are pseudomorphous after coarse primary spinel is substantially lower in Cr# (<0.4) than the primary spinel (Fig. 7). The $Fe^{3+}/(Cr + Al + Fe^{3+})$ atomic ratio is lower than 0.1 in all spinels (Fig. 7). The TiO_2 content is variable but is

Table 1 Selected microprobe analyzes of minerals in peridotite xenoliths from Avacha volcano, the Kamchatka arc, Russia. F-type, fine-grained peridotite

	Primary harzburgite (No. 268)				Primary dunite (No. 161)				Metasomatized (No. 389)				F-type (No. 367)				F-type (No. 159)	
	Ol	Opx-1	Cpx-1	Sp	Ol	Sp	Amph	Ol	Opx-1	Opx-2	Sp	Amph	Ol	Opx-2	Opx-2*	Sp	Ol	Sp
SiO ₂	40.65	58.04	52.90	0.04	41.08	0.00	45.45	41.08	56.13	56.54	0.01	46.68	41.17	57.19	57.59	0.00	40.96	0.11
TiO ₂	0.03	0.00	0.04	0.30	0.00	0.17	0.48	0.04	0.00	0.05	0.02	0.13	0.00	0.00	0.01	0.05	0.02	0.07
Al ₂ O ₃	0.00	1.15	2.31	22.50	0.02	27.78	12.47	0.00	1.64	1.33	13.35	10.03	0.00	1.40	0.90	18.09	0.00	18.70
Cr ₂ O ₃	0.00	0.28	0.53	41.47	0.05	37.23	1.06	0.00	0.32	0.07	53.59	1.96	0.49	0.01	0.00	46.95	0.01	46.93
FeO*	8.60	5.59	2.57	19.44	7.47	18.45	3.90	8.41	5.55	5.20	20.39	3.44	6.08	4.02	4.62	19.49	8.27	20.38
MnO	0.14	0.17	0.09	0.21	0.17	0.28	0.08	0.15	0.10	0.12	0.24	0.07	0.07	0.06	0.12	0.34	0.08	0.09
MgO	49.82	35.36	17.62	14.42	50.47	15.28	19.32	50.49	34.30	34.62	12.66	19.51	51.82	35.92	36.46	13.91	50.05	13.67
NiO	0.37	n.d.	n.d.	n.d.	0.35	n.d.	n.d.	0.38	n.d.	n.d.	n.d.	n.d.	0.41	n.d.	n.d.	n.d.	0.37	n.d.
CaO	0.05	1.00	22.98	0.00	0.08	0.04	11.49	0.05	0.73	0.51	0.02	11.55	0.03	0.14	0.12	0.00	0.03	0.03
Na ₂ O	0.00	0.00	0.20	0.00	0.01	0.00	2.22	0.00	0.00	0.04	0.00	1.90	0.00	0.00	0.01	0.05	0.01	0.03
K ₂ O	0.02	0.00	0.03	0.03	0.02	0.03	0.23	0.00	0.01	0.03	0.05	0.26	0.01	0.04	0.02	0.03	0.03	0.02
Total	99.68	101.59	99.27	98.41	99.72	99.26	96.70	100.60	98.78	98.51	100.33	95.53	100.08	98.78	99.85	98.91	99.83	100.03
Mg#	0.912	0.919	0.924	0.661	0.923	0.679	0.898	0.915	0.917	0.922	0.602	0.910	0.938	0.941	0.934	0.651	0.915	0.632
Cr#				0.553		0.473					0.729					0.635		0.627
Mg/(Cr/)	0.911	0.899	0.495	0.512	0.922	0.444	0.649	0.914	0.904	0.913	0.681	0.656	0.938	0.938	0.932	0.588	0.915	0.581
Fe*/(Al/)	0.088	0.082	0.040	0.414	0.077	0.493	0.073	0.085	0.082	0.077	0.253	0.065	0.062	0.059	0.066	0.338	0.085	0.345
Ca/(Fe ₃₊ /)	0.001	0.019	0.464	0.074	0.001	0.063	0.277	0.001	0.014	0.010	0.066	0.279	0.000	0.003	0.002	0.074	0.000	0.073

Ol, olivine; Opx-1, primary orthopyroxene; Opx-2, secondary orthopyroxene; Opx-2*, secondary radiating orthopyroxene; Cpx, clinopyroxene; Sp, chromian spinel; Amph, amphibole; n.d., not determined. FeO*, total iron as FeO. Mg#, Mg/(Mg + Fe²⁺ + Fe³⁺) atomic ratio; Cr#, Cr/(Cr + Al) atomic ratio; Mg/Fe, fractions of respective cations of (Mg + Fe + Ca) for pyroxenes; Cr/, Al/ and Fe³⁺/, fractions of respective cations of (Cr + Al + Fe³⁺) for chromian spinel. Note that all iron was assumed to be Fe²⁺ in silicates, while Fe²⁺ and Fe³⁺ were calculated for chromian spinel assuming stoichiometry.

generally lower than 0.4 wt% (Table 1). The Mg# has a negative correlation with the Cr# in chromian spinels.

Primary orthopyroxene has high Mg# of around 0.92, being slightly higher than those of coexisting olivine (Table 1). Primary orthopyroxene mostly has 0.5–1.2 wt% of CaO, 1–2 wt% of Al_2O_3 , and 0.2–0.7 wt% of Cr_2O_3 (Fig. 8; Table 1). Secondary orthopyroxenes exhibit compositional varieties depending on the mode of occurrence (Fig. 8). The first type, replacing olivine without associated glass and/or hornblende, is characteristically low both in CaO (typically <0.3 wt%) and Cr_2O_3 (mostly <0.1 wt%; Fig. 8). The second type, replacing olivine and associated with interstitial glass and/or hornblende, is slightly lower in Cr_2O_3 than, but is otherwise almost similar in composition to, the primary one (Fig. 8). The third type, recrystallized from primary orthopyroxene, is almost similar in chemistry to the primary one, but is slightly lower both in CaO, Al_2O_3 and Cr_2O_3 (Fig. 8).

Clinopyroxene is chromian diopside with a high Mg#, ranging from 0.92 to 0.94 (Table 1). The Al_2O_3 content, ranging from 0.8 to 3.5 wt%, is negatively correlated with the Mg#, and the Cr_2O_3 content ranges from 0.5 to 1.1 wt%. Clinopyroxene is extremely poor in TiO_2 , mostly <0.1 wt% (Table 1). The Na_2O content ranges from 0.2 to 0.3 wt% (Table 1). Clinopyroxene associated with the surrounding hornblende selvage is low in Mg# (0.81) and Cr_2O_3 (nil), and is high in Al_2O_3 (4.2 wt%) and TiO_2 (0.52 wt%).

Amphibole is magnesio-hornblende for interstitial or replacement grain within peridotite to tschermakitic hornblende for hornblende selvage, after Leake (1978). Within-peridotite amphibole has a high Mg#, 0.89–0.91, and Cr_2O_3 content, up

to 2 wt%, and has relatively low TiO_2 content, <0.6 wt% (Table 1). Na_2O and K_2O contents of the within-peridotite amphibole are 1.4–2.5 wt% and 0.14–0.26 wt%, respectively (Table 1). In contrast the selvage amphibole has a lower Mg# (down to 0.7) and Cr_2O_3 (down to nil) and a higher TiO_2 (up to 1.9 wt%), and is similar in composition to the phenocrysts in the host andesite.

THERMOBAROMETRY

The two-pyroxene equilibrium temperature (Wells 1977) is approximately 900°C both for unmetasomatized and for strongly metasomatized peridotites. In the unmetasomatized harzburgite the temperature was calculated for pairs of discrete grains of orthopyroxene and associated clinopyroxene. In the strongly metasomatized harzburgite the pair of recrystallized orthopyroxene and associated coarsened clinopyroxene lamella (Fig. 3h) was adopted on calculation. The olivine–spinel geothermometry (Evans & Frost 1975) also indicates similar temperatures (approx. 1000°C) for harzburgites metasomatized to various degrees. Pressure estimation is much more difficult for the refractory spinel peridotite due to lack of a good geobarometer. In the fine-grained metasomatized peridotite relatively aluminous ($\text{Cr}\# < 0.2$) spinel coexists with olivine and pyroxenes, indicating the last equilibration in the spinel lherzolite stability field (Gasparik 1987). This indicates that the Avacha peridotite xenoliths were derived from depths of <60 km, that is, from a shallow half of the mantle wedge around this place.

The redox state of the Avacha peridotite was estimated by the olivine–orthopyroxene–spinel oxygen geobarometer (Ballhaus *et al.* 1990).

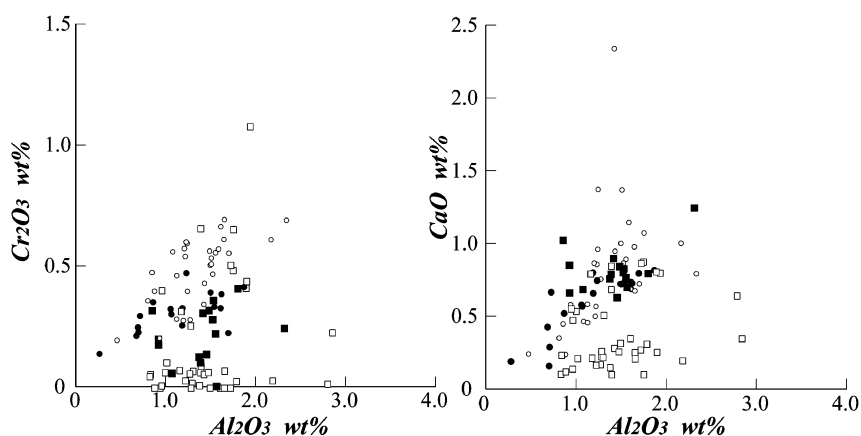


Fig. 8 Compositional variations of orthopyroxenes in peridotite xenoliths from Avacha. Three types of secondary orthopyroxene: (1) replacing olivine without amphibole and/or glass (\square); (2) fine-grained with interstitial amphibole and/or glass (\blacksquare); (3) recrystallized from primary orthopyroxene (\bullet). (\circ), primary.

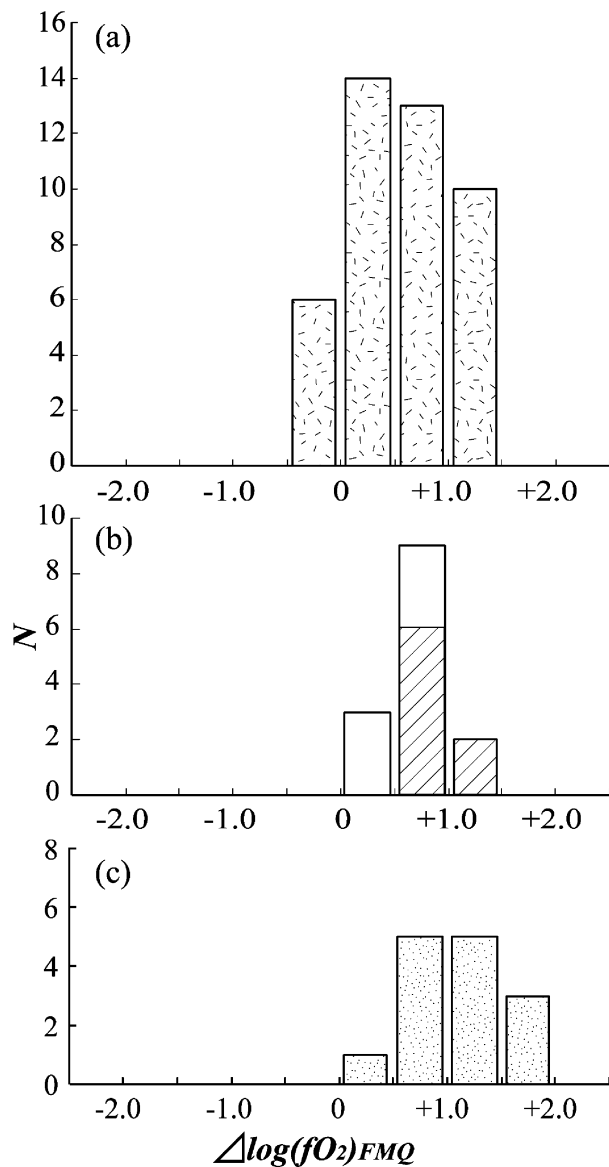


Fig. 9 Frequency histograms of fO_2 (relative to FMQ, ΔFMQ) of peridotite xenoliths from Avacha. The olivine–orthopyroxene–spinel oxygen barometer (Ballhaus *et al.* 1990) was adopted assuming $P = 1.5$ GPa. (a) Primary unmetasomatized peridotite (av. = 0.49). (b) \square , Metasomatized peridotite (av. = 0.68). \boxtimes , vein (av. = 0.83.) Note that ΔFMQ is slightly higher around the vein-like aggregate of secondary orthopyroxene of the 1st type (Fig. 8). (c) Fine-grained peridotite (av. = 0.83).

Assuming tentatively that $P = 1.0$ GPa, we obtain ΔFMQ s (oxygen fugacity relative to the FMQ value) to range from 0 to 2.0 log units (Fig. 9). This range of fO_2 is distinctly higher than the averaged value for abyssal peridotite (Ballhaus *et al.* 1991; Brandon & Draper 1996), and is almost equivalent to the range reported from subarc mantle or its peridotite (Brandon & Draper 1996; Blatter & Carmichael 1998; Parkinson & Arculus 1999). It is

noteworthy that the fO_2 is higher in metasomatized peridotite ($\Delta FMQ = 0.68$ log units on average) than in an apparently unmetasomatized peridotite ($\Delta FMQ = 0.49$ log units on average). In the former peridotite ΔFMQ (0.83 on average) tends to be relatively high around vein-like aggregate of olivine-replacing orthopyroxene (1st type in Fig. 8; Fig. 9b). Fine-grained peridotite yields the highest ΔFMQ (1.06 on average) of all (Fig. 9).

DISCUSSION

The unmetasomatized harzburgite from Avacha has high-Cr# (0.5–0.7) spinel and is more refractory than abyssal peridotites, which have lower-Cr# (<0.6) spinels (Dick & Bullen 1984; Arai 1994a). The Avacha peridotite suite is one of the most refractory mantle materials obtained as xenoliths in basalts and andesites from arcs (Arai 1994a). The refractory harzburgite, like that of the Avacha harzburgite, is a residue after high-degree partial melting assisted by water supply to produce refractory melts that potentially precipitate high-Cr# spinel (Arai 1994b). Such high-Cr# and low-Ti chromian spinel is characteristic of arc magma (Arai 1992). Overall high fO_2 (Fig. 9) is also characteristic of the subarc mantle above subduction zones (Brandon & Draper 1996).

The hornblendite (or gabbro) selvage around peridotite xenolith was formed by the reaction between the peridotite and host andesite. Compositional similarity of hornblende between the selvage and host andesite supports this interpretation. As aforementioned, the attitude of hornblendite (i.e. absence or presence and thickness) does not correlate with any petrographic and mineral chemical characteristics of enclosed peridotite. This strongly indicates that the olivine-replacing orthopyroxene has been formed before the entrapment of peridotite as xenoliths by the magma. We conclude therefore that the metasomatism has occurred within the upper mantle beneath Avacha volcano.

Among various metasomatic effects observed in the mantle wedge the addition of SiO_2 , that is, the formation of orthopyroxene replacing olivine, is one of the most important and fundamental phenomena but has been only recently recognized (Smith *et al.* 1999; Arai & Kida 2000; Smith 2000; McInnes *et al.* 2001; Franz *et al.* 2002). The metasomatic orthopyroxene in peridotite from Avacha replaces olivine in very complicated ways

(Fig. 3c,d), as in the peridotite xenoliths from Iraya volcano (Arai *et al.* 1996). This suggests a very high permeability or very low viscosity of the relevant metasomatic agent. This type of metasomatic orthopyroxene is characteristically free from other metasomatic minerals. In contrast, the secondary metasomatic orthopyroxene forms clear-cut veinlets, replacing olivine along cracks or fractures, in the peridotite xenoliths from Takashima, the South-west Japan arc (Arai *et al.* 2001) or from Tallante, the Betic arc, Spain. The latter type of metasomatic orthopyroxene is characterized by association of other minerals, especially plagioclase and clinopyroxene. This type of metasomatic veinlet comprises the inner filling of plagioclase (and other minerals) and outer metasomatic orthopyroxene lining along the olivine wall. This indicates the higher viscosity of the metasomatic agent for this type of orthopyroxene formation than for the former type. Melts with relatively low permeability or high viscosity could effectively move only through cracks. We suggest that the metasomatic agent for the Avacha-type orthopyroxene formation was aqueous fluid, and that for the Takashima-type orthopyroxene it was silicate melt. The main solute for the former was silica, resulting in the sole formation of orthopyroxene by replacing olivine. The latter is expected to have had appreciable amounts of other components in addition to silica, resulting in the precipitation of plagioclase and clinopyroxene in addition to orthopyroxene. This is

possible because SiO_2 is more partitioned to fluids than other components (e.g. CaO and Al_2O_3) at some conditions (Eggler 1987).

The type of metasomatism recorded by peridotite xenoliths is quite different between the Valovayan Volcanic Field, the north Kamchatka arc (Kepezhinskias *et al.* 1995) and Avacha volcano, the south Kamchatka arc (present study). The metasomatic agent of the former was silicate melts that precipitated largely pyroxenites (Kepezhinskias *et al.* 1995). The subduction style is clearly different between the northern and southern parts of the Kamchatka arc. As Kepezhinskias *et al.* (1995) suggested, slab melting had occurred by subduction of the hot oceanic crust of the Komandorsky Basin (Baranov *et al.* 1991) beneath the north Kamchatka arc. The slab melts were adakitic in nature and had formed pyroxenites within the mantle wedge and simultaneously given rise to Na-metasomatism to the surrounding peridotite. In the south Kamchatka arc, in contrast, the subducting slab has been too cool to lead to slab melting and could only discharge hydrous fluids or supercritical fluids rich in H_2O , which has precipitated mainly orthopyroxene at the expense of olivine within the upper mantle. The secondary orthopyroxene with similar textural characteristics from other arcs (e.g. Papua New Guinea, Iraya and Colorado Plateau) has similar chemical features; that is, low contents of CaO , Cr_2O_3 and, sometimes, Al_2O_3 (Fig. 10).

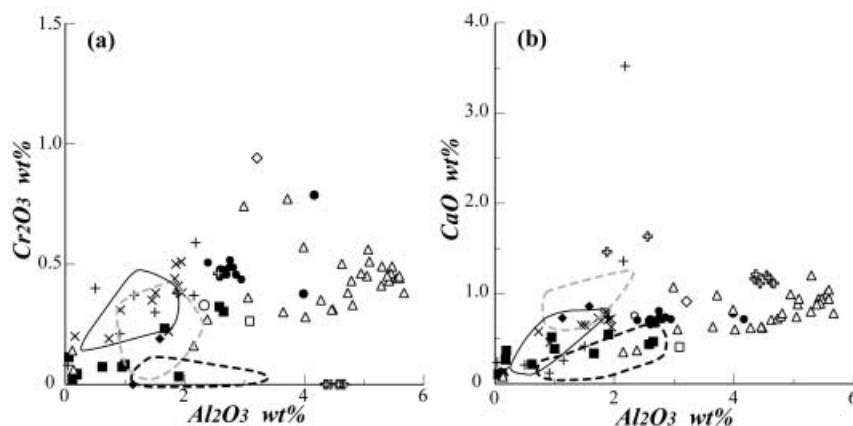


Fig. 10 Comparison of orthopyroxene compositions between the Avacha peridotites and other peridotite xenoliths derived from arcs and related settings. Three types of secondary orthopyroxene (see text) in Avacha peridotites are indicated by three areas for their main clusters (Fig. 8). Note that the secondary orthopyroxenes tend to be lower in Ca, Al and Cr than the primary orthopyroxenes on average. Data source: Papua New Guinea (McInnes *et al.* 2001; Franz *et al.* 2002); Colorado Plateau (Smith & Riter 1997; Smith *et al.* 1999; Smith 2000); Cascade Range (Draper 1992; Brandon & Draper 1996; Ertan & Leeman 1996); Mexico (Luhr & Aranda-Gomez 1997; Blatter & Carmichael 1998); Philippines (Iraya (Arai & Kida 2000); and North Kamchatka (Kepezhinskias *et al.* 1995). Primary: (×), Papua New Guinea; (□), Colorado Plateau; (○), Cascade; (◇), Philippines; (△), Mexico. (⊕), North Kamchatka (Valovayam Volcanic Field). Secondary: (+), Papua New Guinea; (■) Colorado Plateau; (●) Cascade; (◆), Philippines. Avacha: (- - -), 1st type, olivine-replacing; (- · - ·), 2nd type, fine grained; (—), 3rd type, recrystallized.

The mantle wedges have suffered silica enrichment by addition both of melts and of hydrous fluids from subducting slabs. Whether the metasomatic agent supplied is silicate melt or aqueous fluid depends on the thermal state of the slab. Kelemen *et al.* (1998) ascribed the enrichment of orthopyroxene in cratonic mantle peridotites to silica addition through a melt/peridotite reaction during the mantle-wedge stage. The metasomatized harzburgite could have become subcratonic harzburgite if enrolled by subduction flows into the deeper mantle (Kelemen *et al.* 1998). The observation of the Avacha peridotite xenoliths derived from the mantle wedge of the Kamchatka arc supports their conclusion. The metasomatized harzburgite with olivine of Fo₉₁₋₉₂ from Avacha contains 40 vol% of total orthopyroxene on average. This is equivalent to some subcratonic harzburgite (Boyd 1989), and can be orthopyroxene-rich refractory harzburgite if homogenized through recrystallization.

CONCLUSIONS

Peridotite xenoliths from Avacha volcano, the south Kamchatka arc, are predominantly harzburgite. The harzburgite for Avacha is refractory, having nil or a small amount of clinopyroxene. Olivine is Fo₉₁₋₉₂ and the Cr# of spinel ranges from 0.5 to 0.7.

The peridotite xenoliths commonly suffer severe metasomatism to produce secondary orthopyroxene at the expense of olivine. The secondary orthopyroxene is free of deformation and exsolution, and is mostly poor in CaO and Cr₂O₃. The *f*O₂ is higher in metasomatized harzburgite than in the unmetasomatized harzburgite, indicating the oxidizing conditions of metasomatism.

The texture of the secondary orthopyroxene indicates the high permeability or mobility of the metasomatic agent, that is, hydrous fluid rather than silicate melt. The subducting slab beneath the southern part of the Kamchatka arc is too cool to produce slab melts and has released only hydrous fluids to the mantle wedge.

The metasomatized harzburgite from Avacha contains approximately 40 vol% of orthopyroxene on average. This enrichment of orthopyroxene or silica has been continuous in time within mantle wedges above subducting slabs. If the metasomatized harzburgite had been transported to the deeper mantle, it could have become one of the constituents of the subcratonic mantle.

ACKNOWLEDGEMENTS

We are grateful to K. Kadoshima for his assistance in microprobe analysis and collaboration in the field. K. Koyanagi also helped us to collect samples in the field. T. Morishita, Y. Shimizu and J. Uesugi assisted one of us (SI) in microprobe analysis. We are indebted to T. Fujii, S. Banno and an anonymous reviewer for their comments, which were helpful in revision of the manuscript.

REFERENCES

- AOKI K. 1987. Japanese Island arc: xenoliths in alkali basalts, high-alumina basalts, and calc alkaline andesites and dacites. In Nixon P. H. (ed.), *Mantle Xenoliths*, pp. 319–33. John Wiley & Sons, New York.
- ARAI S. 1992. Chemistry of chromian spinel in volcanic rocks as a potential guide to magma chemistry. *Mineralogical Magazine* **56**, 173–84.
- ARAI S. 1994a. Characterization of spinel peridotites by olivine–spinel compositional relationships: Review and interpretation. *Chemical Geology* **111**, 191–204.
- ARAI S. 1994b. Compositional variation of olivine–chromian spinel in Mg-rich magmas as a guide to their residual spinel peridotites. *Journal of Volcanology and Geothermal Research* **59**, 279–94.
- ARAI S., ABE N., HIRAI H. & SHIMIZU Y. 2001. Geological, petrographical and petrological characteristics of ultramafic–mafic xenoliths in Kurose and Takashima, northern Kyushu, southwestern Japan. *Science Reports of Kanazawa University* **46**, 9–38.
- ARAI S., HIRAI H. & ABE N. 1998. Petrological characteristics of the sub-arc mantle: An overview on petrology of peridotite xenoliths from the Japan arc. *Trends in Mineralogy (India)* **2**, 39–55.
- ARAI S. & KIDA M. 2000. Origin of fine-grained peridotite xenoliths from Iraya volcano of Batan Island, Philippines: Deserpentinization or metasomatism at the wedge mantle beneath an incipient arc? *The Island Arc* **9**, 458–71.
- ARAI S., KIDA M., ABE N., NINOMIYA A. & YUMUL G. P. Jr. 1996. Classification of peridotite xenoliths in calc-alkaline andesite from Iraya volcano, Batan Island, the Philippines, and its genetical implications. *Science Reports of Kanazawa University* **41**, 25–45.
- BALLHAUS C., BERRY R. F. & GREEN D. H. 1990. Oxygen fugacity controls in the Earth's upper mantle. *Nature* **348**, 437–40.
- BALLHAUS C., BERRY R. F. & GREEN D. H. 1991. High pressure experimental calibration of the olivine–orthopyroxene–spinel oxygen geobarometer: Implications for the oxidation state of the upper mantle. *Contributions to Mineralogy and Petrology* **107**, 27–40.

- BARANOV B. V., SELIVERSTOV N. I., MURAVIEV A. V. & MUZUROV E. L. 1991. Commander Basin: Product of a back-transform spreading. *Tectonophysics* **199**, 237–69.
- BLATTER D. L. & CARMICHAEL I. S. E. 1998. Hornblende peridotite xenoliths from central Mexico reveal the highly oxidized nature of subarc upper mantle. *Geology* **26**, 1035–8.
- BOYD F. R. 1989. Compositional distinction between oceanic and cratonic lithosphere. *Earth and Planetary Science Letters* **96**, 15–26.
- BRAITSEVA O. A., BAZONOVA L. I., MELEKESTSEV I. V. & SULERZHINTSKIY L. D. 1998. Large Holocene eruptions of Avacha volcano, Kamchatka (7250–3700 ¹⁴C years B.P.). *Volcanology and Seismology* **20**, 1–27.
- BRANDON A. D. & DRAPER D. S. 1996. Constraints on the origin of the oxidation state of mantle overlying subduction zones: An example from Simcoe, Washington, USA. *Geochimica et Cosmochimica Acta* **60**, 1739–49.
- DICK H. J. B. & BULLEN T. 1984. Chromian spinel as a petrogenetic indicator in abyssal and alpine-type peridotites and spatially associated lavas. *Contributions to Mineralogy and Petrology* **86**, 54–76.
- DRAPER D. S. 1992. Spinel lherzolite xenoliths from Lorena Butte, Simcoe Mountains, southern Washington (USA). *Journal of Geology* **100**, 766–76.
- EGGLER D. H. 1987. Solubility of major and trace elements in mantle metasomatic fluids: Experimental constraints. In Menzies M. A. & Hawkesworth C. J. (eds). *Mantle Metasomatism*, pp. 21–41. Academic Press, London.
- ERTAN I. E. & LEEMAN W. P. 1996. Metasomatism of Cascades subarc mantle: Evidence from a rare phlogopite orthopyroxenite xenolith. *Geology* **24**, 451–4.
- EVANS B. W. & FROST B. R. 1975. Chrome–spinel in progressive metamorphism: A preliminary analysis. *Geochimica et Cosmochimica Acta* **39**, 959–72.
- FRANZ L., BECKER K.-P., KRAMER W. & HERZIG P. M. 2002. Metasomatic mantle xenoliths from the Bismarck microplate (Papua New Guinea): Thermal evolution, geochemistry and extent of slab-induced metasomatism. *Journal of Petrology* **43**, 315–43.
- GASPARIK T. 1987. Orthopyroxene thermometry in simple and complex systems. *Contributions to Mineralogy and Petrology* **96**, 357–70.
- IVANOV B. V., FLEROV G. B., MASURENKOV YU. P. *et al.* 1996. The 1991 eruption of Avacha volcano: Dynamics and the composition of eruptive products. *Volcanology and Seismology* **17**, 369–94.
- KELEMEN P. B., HART S. R. & BERNSTEIN S. 1998. Silica enrichment in the continental upper mantle via melt/rock reaction. *Earth and Planetary Science Letters* **164**, 387–406.
- KEPEZHINSKAS P. K., DEFANT M. J. & DRUMMOND M. S. 1995. Na metasomatism in the island-arc mantle by slab melt–peridotite interaction: evidence from mantle xenoliths in the north Kamchatka arc. *Journal of Petrology* **36**, 1505–27.
- KEPEZHINSKAS P. K., DEFANT M. J. & DRUMMOND M. S. 1996. Progressive enrichment of island arc mantle by melt–peridotite interaction inferred from Kamchatka xenoliths. *Geochimica et Cosmochimica Acta* **60**, 1217–29.
- KOLOSOKOV A. V. & KHOTIN M. YU. 1978. Ultramafic inclusions in lavas of present Kamchatka volcanoes. In Academy of Sciences of the USSR Soviet Geophysical Committee (eds). *Inclusions in the Volcanic Rocks of the Kuril-Kamchatka Island Arc*, pp. 36–66. Nauka, Moscow (in Russian with English abstract).
- LEAKE B. E. 1978. Nomenclature of amphiboles. *American Mineralogist* **63**, 1023–52.
- LUHR J. F. & ARANDA-GOMEZ J. J. 1997. Mexican peridotite xenoliths and tectonic terranes: Correlations among vent location, texture, temperature, pressure, and oxygen fugacity. *Journal of Petrology* **38**, 1075–112.
- MCINNES B. I. A., GREGOIRE M., BINNS R. A., HERZIG P. M. & HANNINGTON M. D. 2001. Hydrous metasomatism of oceanic sub-arc mantle, Lihir, Papua New Guinea: petrology and geochemistry of fluid-metasomatised mantle wedge xenoliths. *Earth and Planetary Science Letters* **188**, 169–83.
- MAURY R. C., DEFANT M. J. & JORON J.-L. 1992. Metasomatism of the sub-arc mantle inferred from trace elements in Philippine xenoliths. *Nature* **360**, 661–3.
- MELEKESTSEV I. V., SULERZHINTSKIY L. D., BAZONOVA L. I., BRAITSEVA O. A. & FLORENSKAYA L. I. 1996. Holocene catastrophic lahars at Avacha and Koryakskiy volcanoes in Kamchatka. *Volcanology and Seismology* **17**, 561–70.
- NINOMIYA A. & ARAI S. 1992. Harzburgite fragment in a composite xenolith from an Oshima–Oshima andesite, the Northeast Japan arc. *Bulletin of the Volcanological Society of Japan* **37**, 269–73.
- NIXON P. H. 1987. *Mantle Xenoliths*. John Wiley & Sons, New York.
- PARKINSON I. J. & ARCULUS R. J. 1999. The redox state of subduction zone: Insights from arc peridotites. *Chemical Geology* **160**, 409–23.
- ROSS C. S., FOSTER M. D. & MYERS A. T. 1954. Origin of dunites and olivine-rich inclusions in basaltic rocks. *American Mineralogist* **39**, 693–737.
- SCHIANO P., CLOCCHIATTI R., SHIMIZU N., MAURY R. C., JOCHUM K. P. & HOFMANN A. W. 1995. Hydrous, silica rich melts in the sub-arc mantle and their relationship with erupted arc lavas. *Nature* **377**, 595–600.
- SHCHEKA S. A. 1976. Evidence of metamorphism of ultramafic inclusions before incorporation into basalt magma. *Doklady of Akademy Nauk SSSR* **227**, 704–7.
- SMITH D. 2000. Insights into the evolution of the uppermost continental mantle from xenolith localities on and near the Colorado Plateau and regional compar-

- isons. *Journal of Geophysical Research* **105**, 16769–81.
- SMITH D. & RITER J. C. A. 1997. Genesis and evolution of low-Al orthopyroxene in spinel peridotite xenoliths, Grand Canyon field, Arizona, USA. *Contributions to Mineralogy and Petrology* **127**, 391–404.
- SMITH D., RITER J. C. A. & MERTZMAN S. A. 1999. Erratum to 'Water-rock interactions, orthopyroxene growth and Si-enrichment in the mantle: Evidence in xenoliths from the Colorado Plateau, southwestern United States'. *Earth and Planetary Science Letters* **167**, 347–56.
- TAKAHASHI E. 1978. Petrologic model of the crust and upper mantle of the Japanese island arcs. *Bulletin Volcanologique* **41**, 529–47.
- TATSUMI Y., FURUKAWA Y., KOGISO T., YAMANAKA Y., YOKOYAMA T. & FEDOTOV S. A. 1994. A third volcanic chain in Kamchatka: Thermal anomaly at transform/convergence plate boundary. *Geophysical Research Letters* **21**, 537–40.
- WELLS P. R. A. 1977. Pyroxene thermometry in simple and complex systems. *Contributions to Mineralogy and Petrology* **62**, 129–39.